Supplementary Information (SI) for Journal of Materials Chemistry C.
This journal is © The Royal Society of Chemistry 2025

ESIPT-Suppressed *2-(2'-hydroxyphenyl)benzoxazole* derivative as a new photoinitiator for multiphoton polymerization

João V. P. Valverde[a], André L. S. Romero[a], Renan Cunha[a], Rafael Q. Garcia[a], Timothée Stoerkler[b], Julien Massue[b], Leonardo De Boni[a] and Cleber R. Mendonça[a,*]

[a] *São Carlos Institute of Physics, University of São Paulo, CP 369, 13560-970 São Carlos, SP, Brazil*
[b] *Institut de Chimie et Procédés pour l'Energie, l'Environnement et la Santé (ICPEES), Université de Strasbourg, UMR CNRS 7515, 67087 Strasbourg Cedex 02, France*

*Author to whom correspondence should be addressed: crmendon@ifsc.usp.br and joaovalverde@ifsc.usb.br

Supplementary Information

SI1. Linear photophysical properties

To determine the linear photophysical properties, **HBO-NBu$_2$** was dissolved in dichloromethane (DCM) at a concentration of approximately $10.0^{-5}\ mol/L$ and placed it in a quartz cell with a $10.0\ mm$ path length. We collected the one-photon absorption (1PA) and fluorescence spectra using a UV-Vis spectrophotometer (UV-1800 model, Shimadzu) and a spectrofluorometer (F-7000 model, Hitachi), respectively. For the fluorescence measurements, we adjusted the solution concentration to an absorbance of approximately 0.5 to minimize fluorescence reabsorption. We determined the fluorescence quantum yield (ϕ_{fl}) using the well-known Brouwer method[1,2], with coumarin 500 dissolved in methanol ($\phi_{fl} = 68.1\%$)[3] as the standard sample. We performed solvatochromism measurements by dissolving the molecule in different solvents, namely toluene, tetrahydrofuran (THF), dichloromethane (DCM), dimethylsulfoxide (DMSO), dimethylformamide (DMF), ethanol, acetonitrile (ACN), and methanol (see **Figs. SI1a**, **SI1b**, and **SI1c**). The solvatochromism measurement and the Lippert-Mataga equation[4,5] allowed us to determine the difference between the permanent dipole moment of the excited state and the ground one ($|\Delta\vec{\mu}|$)[6]. Finally, we measured the excitation anisotropy spectrum using the L-configuration[7], in which we polarize the excitation and fluorescence emission beams in different directions (specifically in vertical and horizontal polarization combinations).

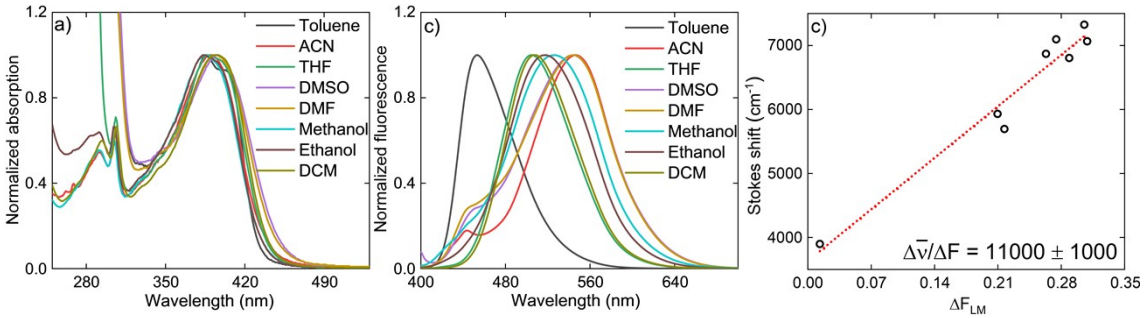

Figure SI1 – a,b) Normalized absorbance and fluorescence spectra in different solvents, and c) Stokes shift *versus* the Lippert–Mataga polarity function.

SI2. Measurement of two- and three-photon absorption

We measured the two- and three-photon absorption (2PA and 3PA) spectrum using the multiphoton-excited fluorescence (MPEF) technique[8–10]. This method directly compares the fluorescence intensity excited by multiphoton absorption (MPA) with that of 1PA, using the latter to calibrate detection efficiency and, consequently, ϕ_{fl}. Thus, we determined the 2PA and 3PA cross-sections (σ_{2PA} and σ_{3PA}) by comparing the multiphoton excited fluorescence signal with the one-photon excited one, ensuring detection under identical experimental conditions. We obtained σ_{2PA} and σ_{3PA} using the following equations[8]:

$$\sigma_{2PA} = \frac{1}{\sqrt{2}}\left(\frac{\pi}{\ln(2)}\right)^{\frac{3}{2}} \frac{P_{1PA}(h\nu_{2PA})^2 F_{2PA}}{P_{2PA}\ h\nu_{1PA}\ F_{1PA}} (T\tau\Delta x\Delta y)\left(\frac{1-10^{-Abs(\lambda_{1PA})}}{Abs(\lambda_{1PA})\cdot ln(10)}\right)\sigma_{1PA}(\lambda_{1PA}), \quad (1)$$

and

$$\sigma_{3PA} = 3\left(\frac{\sqrt{3}\,\pi}{4\ln(2)}\right)^{3} \frac{P_{1PA}\ (h\nu_{3PA})^3 F_{3PA}}{(P_{3PA})^3\ h\nu_{1PA}\ F_{1PA}} (T\tau\Delta x\Delta y)^2\left(\frac{1-10^{-Abs(\lambda_{1PA})}}{Abs(\lambda_{1PA})\cdot ln(10)}\right)\sigma_{1PA}(\lambda_{1PA}). \quad (2)$$

In this equation, P_{nPA} represents the average power of the beam laser, $h\nu_{nPA}$ is the photon energy, and F_{nPA} is the fluorescence signal. The subscript nPA refers to *n*-photon excitation, where n can be 1, 2, or 3. T denotes the laser repetition rate, τ is the pulse duration (FWHM), and Δx and Δy represent the spatial width (FWHM) of the beam laser. Additionally, σ_{1PA} and Abs indicate the 1PA cross-section and the absorbance at the specific 1PA wavelength, respectively.

The experimental setup of the MPEF technique consists of a regenerative amplified Yb:KGW femtosecond laser system (Pharos PH1 model, Light Conversion,

Inc.) with the following specifications: $800\ \mu J$ pulse energy, with $220\ fs$ pulse width, centered at $1030\ nm$, and repetition rate of $7.5\ kHz$. We used this laser system to pump an optical parametric amplifier (OPA) (Orpheus model, Light Conversion, *Inc.*). The OPA, combined with two second- and fourth-harmonic generation systems (Lyra-FH model, Light Conversion, *Inc.*), allows us to generate tunable pulses from $220 - 3000\ nm$, with pulse energies between 0.07 and $67\ \mu J$ and $100 - 180\ fs$ pulse width, characterized by an autocorrelator (GECO model, Light Conversion, *Inc.*). Below, we give a brief description of the experimental setup.

In our setup, we initially direct the beam emerging from the OPA to a spatial filter, using dichroic mirrors to eliminate residual wavelengths. The spatial filter generates a Gaussian intensity profile beam for all excitation wavelengths. We then align the excitation beam by 1PA, 2PA, and 3PA through two pinholes placed before and after the sample. This alignment ensures we collect the fluorescence signal under the same experimental conditions. We focused the laser beam on the sample using a $f = 25$ cm lens, positioned $8\ cm$ before the focal point. A beam splitter between the lens and the sample cell directs $< 4\%$ of the laser beam to a CCD camera to determine Δx and Δy. We collect the fluorescence signal perpendicular to the excitation beam, using the combination of two $f = 5cm$ lenses and a $R = 10\ cm$ spherical mirror, and focus the horizontally-elongated fluorescence image on the entrance plane of a monochromator. We coupled a photomultiplier tube to the monochromator, connected to a lock-in amplifier, and triggered it with the laser repetition rate to detect the fluorescence emission signal. Finally, we obtain the fluorescence signal from the average of 10 acquisitions, each with an integration time of $1\ s$.

We performed the 3PA measurement as described above, with the difference that, in this case, we focused the laser beam more strongly on the sample, positioned $5\ cm$ before the focal point.

We have taken all the precautions as discussed by Makarov *et al.*[8], including keeping the monochromator slit opening the same 1PA, 2PA, and 3PA measurements. The photomultiplier voltage, integration time, and lock-in amplification are the same in all three situations. Furthermore, we have eliminated any spurious signals, such as laser scattering. Regarding sample preparation, we placed the solution in a quartz cell with a $10\ mm$ path length at the same concentration mentioned for 1PA. Finally, one performed

2PA measurements in the $550 - 900\ nm$ range with a spectral resolution of $10\ nm$ and by 3PA at $1030\ nm$.

SI3. Femtosecond transient absorption spectroscopy

We performed femtosecond transient absorption (TA) measurements using a homemade pump-probe setup based on the same laser system and OPA described in the previous section (at a repetition rate of $\sim 1.9\ kHz$). In this setup, we split the laser system beam using a 50% beam splitter. We use one of the beams to pump the OPA, generating a tunable pump pulse at $400\ nm$ ($\sim 100\ fs$). We attenuate the second beam power (4.0 mW) to generate a white-light continuous probe pulse ($450 - 1030\ nm$) by focusing the beam onto a $2.0\ mm$ thick sapphire window. We then focus both beams on the sample (spatially overlapping) and collect the spectrum of the transmitted probe pulse with a portable spectrometer (USB2000+ model, Ocean Optics). We vary the probe-probe time delay via a computer-controlled translation stage. We performed the measurements under magic angle polarization conditions ($54.7°$). Finally, we conducted the global analysis of the TA spectra using a custom-developed program, applying the methodology described by Van Stokkum *et al*.[11].

SI4. Time-resolved fluorescence

We determined the fluorescence lifetime (τ_{fl}) of the **HBO-NBu$_2$** molecule by the time-resolved fluorescence technique using the same laser system and OPA described above (at a repetition rate of $300\ Hz$). We excited the sample at $400\ nm$ and monitored the fluorescence signal as a function of the time. We obtained τ_{fl} by the signal convolution method[12], which convolutes the IRF with a monoexponential decay function[6].

SI5. Quantum chemical calculations

To better understand the properties of **HBO-NBu$_2$**, we performed quantum chemical calculations (QCC) based on the framework of density functional theory (DFT) and its time-dependent extension (TD-DFT), employing the Gaussian 09 software[13]. First, we conducted geometry optimization and vibrational frequency calculations using the hybrid functional M06-2X[14] and Pople's standard 6-311G(d,p) basis set[15]. We did not identify negative vibrational modes, indicating that the fully optimized structure

corresponds to a stable minimum. We then performed TD-DFT calculations to determine the 20 lowest-energy singlet electronic transitions, employing the hybrid functional B3LYP[16] and the Pople's extended 6-311G++(d,p) basis set. With the same methodology, we also calculated the molecular orbitals and Le Bahers' parameters[17], such as effective charge displacement length ($^{D}_{CT}$), transferred charge ($^{q}_{CT}$) and $|\Delta\vec{\mu}|$. We performed all QCC considering DCM as the solvent medium by using the Polarizable Continuum Model (PCM) with integral equation formalism (IEF-PCM)[18,19]. We summarize in **Table SI1** and **SI2** the optimized molecular geometry (equilibrium) and electronic transition data of **HBO-NBu$_2$**, respectively.

Table SI1 – Optimized structures of **HBO-NBu$_2$** obtained through IEFPCM-M062x/6-311G(d,p) calculations in DCM medium.

HBO-NBu$_2$			
IEFPCM-TD-M062x/6-311G(d,p)			
C	10.5684	-0.7757	0.7784
C	10.6737	0.1834	-0.2407
C	9.5509	0.7341	-0.8444
C	8.3095	0.2922	-0.3932
C	8.2313	-0.6615	0.6201
C	9.3335	-1.2240	1.2360
N	7.0108	0.6262	-0.7682
C	6.2461	-0.0982	-0.0093
O	6.9062	-0.9046	0.8583
C	4.7961	-0.1153	-0.0119
C	4.0950	0.7217	-0.9050
C	2.7010	0.7019	-0.9033
C	2.0042	-0.1333	-0.0319
C	2.7060	-0.9678	0.8584
C	4.0841	-0.9505	0.8596
C	0.5755	-0.1428	-0.0428
C	-0.6321	-0.1567	-0.0476
C	-2.0610	-0.1706	-0.0532
C	-2.7777	0.6475	-0.9382
C	-4.1622	0.6212	-0.9492

C	-4.8728	-0.2064	-0.0730
C	-4.1547	-1.0191	0.8118
C	-2.7676	-1.0079	0.8185
N	-6.2974	-0.1913	-0.1130
C	-7.0286	4.7478	0.7046
C	-7.3368	3.3131	1.1260
C	-6.5756	2.2877	0.2865
C	-6.8736	0.8643	0.7397
C	-10.2321	-3.1733	-1.0236
C	-8.9002	-3.0061	-0.2960
C	-8.2653	-1.6410	-0.5560
C	-6.9237	-1.4918	0.1556
H	11.4712	-1.1779	1.2205
H	11.6579	0.5002	-0.5625
H	9.6278	1.4739	-1.6305
H	9.2368	-1.9624	2.0203
H	2.1741	1.3485	-1.5930
H	2.1595	-1.6137	1.5321
H	4.6371	-1.5869	1.5390
H	-2.2384	1.2884	-1.6250
H	-4.7170	1.2308	-1.6518
H	-4.6836	-1.6664	1.5014
H	-2.2211	-1.6431	1.5050
H	-7.5821	5.4695	1.3080
H	-7.2952	4.9094	-0.3430
H	-5.9628	4.9637	0.8146
H	-8.4123	3.1263	1.0391
H	-7.0811	3.1769	2.1821
H	-5.5035	2.4940	0.3581
H	-6.8538	2.3905	-0.7681
H	-6.5375	0.7300	1.7823
H	-7.9568	0.7235	0.7337
H	-10.6726	-4.1535	-0.8318

H	-10.0990	-3.0691	-2.1034
H	-10.9484	-2.4132	-0.7012
H	-8.2069	-3.7929	-0.6117
H	-9.0500	-3.1371	0.7809
H	-8.9604	-0.8582	-0.2364
H	-8.1042	-1.5024	-1.6297
H	-7.0558	-1.6612	1.2372
H	-6.2531	-2.2723	-0.2124
O	4.7052	1.5471	-1.7678
H	5.6760	1.4616	-1.6656

136

137 **Table SI2** – Theoretical photophysical properties of **HBO-NBu$_2$** molecule obtained by IEFPCM-TD-
138 B3LYP/6-311++G(d,p) calculation in DCM medium, such as electronic state, transition energy, transition
139 wavelength, and oscillator strength.

HBO-NBu$_2$ IEFPCM-TD-B3LYP/6-311++G(d,p)			
Electronic state	Energy (eV)	Wavelength (nm)	Oscillator Strength
S_0-S_1	3.1647	391.77	1.5185
S_0-S_2	3.6818	336.75	0.3616
S_0-S_3	4.0260	307.96	0.1658
S_0-S_4	4.2857	289.30	0.0847
S_0-S_5	4.3659	283.98	0.0034
S_0-S_6	4.4335	279.65	0.0119
S_0-S_7	4.4599	278.00	0.0157
S_0-S_8	4.6161	268.59	0.0000
S_0-S_9	4.6960	264.02	0.0331
S_0-S_{10}	4.7474	261.16	0.0217
S_0-S_{11}	4.8511	255.58	0.0243
S_0-S_{12}	5.0113	247.41	0.0239
S_0-S_{13}	5.0472	245.65	0.0019
S_0-S_{14}	5.1138	242.45	0.0089
S_0-S_{15}	5.1996	238.45	0.0065
S_0-S_{16}	5.2193	237.55	0.0242

S_0-S_{17}	5.2453	236.37	0.0158
S_0-S_{18}	5.2764	234.98	0.0652
S_0-S_{19}	5.3469	231.88	0.0150
S_0-S_{20}	5.3782	230.53	0.0044

SI6. Multiphoton polymerization

We employed a homemade setup to investigate the viability of **HBO-NBu$_2$** as a photoinitiator for MPP. Depending on the absorption process, we used two different laser systems. For 2PP, we used an amplified femtosecond erbium laser system (FemtoFiber Scientific model, Toptica Photonics, *Inc*.) with a $200\ fs$ pulse width at $775\ nm$ (second harmonic of $1550\ nm$), operating at a repetition rate of $80\ MHz$ ($0.75\ nJ/pulse$). For 3PP, we used an amplified Yb:KGW femtosecond laser system (Carbide, Light Conversion, *int*.) with a $244\ fs$ pulse width at $1030\ nm$ and operating at a repetition rate of $1\ MHz$ ($5.0\ \mu J/pulse$). We directed the beam to a rotating polarizer and a half-wave plate to control the excitation power. We focused the beam onto the sample with an objective lens ($62\times$, $NA = 0.80$) and positioned the sample on a computer-controlled x-y-z translation stage, set at a writing speed of $20\ \mu m/s$. We adjusted the incident power from 6 to $14\ mW$ (0.075 to $0.18\ nJ$) for 2PA and used a fixed power of $6.0\ mW$ ($6\ nJ$) for 3PA.

The sample used here consists of a mixture of two commercial acrylic resins, *ethoxylated(6)trimethylolpropane triacrylate* (SR499 – Sartomer) and *tris(2-hydroxyethyl)isocyanurate triacrylate* (SR368 – Sartomer) (see **Fig. SI2**), employed in equal mass proportions ($wt\%$). This combination provides mechanical stability to the final structure and minimizes shrinkage after polymerization[20]. We incorporated different concentrations of **HBO-NBu$_2$**, previously dissolved in DCM (0.01 to $0.08\ wt\%$). After solvent evaporation, we placed a small sample drop on a glass substrate with a micrometric spacer and covered it with a coverslip. After completing the microfabrication process, we washed the samples by immersing them in ethanol heated to 75 °C for 15 min. We repeated this procedure three times to ensure the complete removal of residues.

a)

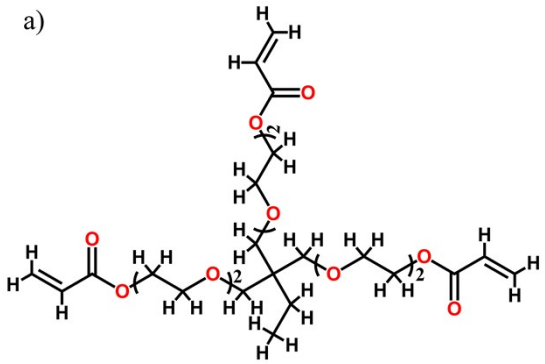

SR499 – *ethoxylated(6)trimethylolpropane triacrylate*

b)

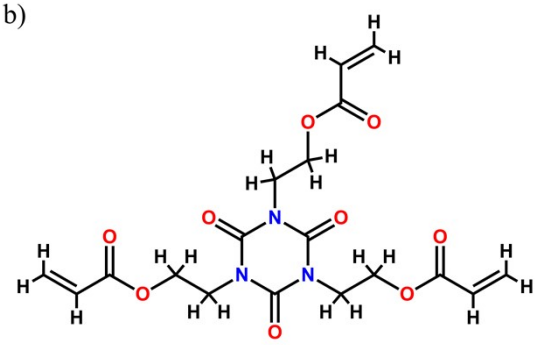

SR368 – *tris(2-hydroxyethyl)isocyanurate triacrylate*

Figure SI2 – Representation of the chemical structure of the monomers: a) ethoxylated(6) trimethylolpropane triacrylate (**SR499** – Sartomer) and b) tris(2-hydroxyethyl) isocyanurate triacrylate (**SR368** – Sartomer).

SI7. REFERENCES

1 A. M. Brouwer, 2011, preprint, DOI: 10.1351/PAC-REP-10-09-31.

2 U. Resch-Genger and P. C. DeRose, *Pure and Applied Chemistry*, 2010, **82**, 2315–2335.

3 L. S. Rohwer and J. E. Martin, *J Lumin*, 2005, **115**, 77–90.

4 E. Lippert, *Zeitschrift für Elektrochemie, Berichte der Bunsengesellschaft für physikalische Chemie*, 1957, **61**, 962–975.

5 N. Mataga, Y. Kaifu and M. Koizumi, *Bull Chem Soc Jpn*, 1956, **29**, 465–470.

6 L. H. Zucolotto Cocca, J. V. P. Valverde, J. le Bescont, C. Breton-Patient, S. Piguel, D. L. Silva, C. R. Mendonca and L. De Boni, *J Mol Struct*, 2024, **1300**, 137221.

7 Joseph R. Lakowicz, in *Principles of Fluorescence Spectroscopy*, ed. J. R. Lakowicz, Springer US, Boston, MA, 2006, pp. 353–382.

8 N. S. Makarov, M. Drobizhev and A. Rebane, *Opt Express*, 2008, **16**, 4029.

9 C. Xu and W. W. Webb, *Measurement of two-photon excitation cross sections of molecular fluorophores with data from 690 to 1050 nm*, 1996, vol. 13.

10 S. de Reguardati, J. Pahapill, A. Mikhailov, Y. Stepanenko and A. Rebane, *Opt Express*, 2016, **24**, 9053.

11 I. H. M. Van Stokkum, D. S. Larsen and R. Van Grondelle, *Elsevier*, 2004, preprint, DOI: 10.1016/j.bbabio.2004.04.011.

12 C. B. Talbot, J. Lagarto, S. Warren, M. A. A. Neil, P. M. W. French and C. Dunsby, *J Fluoresc*, 2015, **25**, 1169–1182.

13 M. J. Frisch, G. W. Trucks, H. B. Schlegel, G. E. Scuseria, M. A. Robb, J. R. Cheeseman, G. Scalmani, V. Barone, G. A. Petersson, H. Nakatsuji, X. Li, M. Caricato, A. Marenich, J. Bloino, B. G. Janesko, R. Gomperts, B. Mennucci, H. P. Hratchian, J. V. Ortiz, A. F. Izmaylov, J. L. Sonnenberg, D. Williams-Young, F. Ding, F. Lipparini, F. Egidi, J. Goings, B.

Peng, A. Petrone, T. Henderson, D. Ranasinghe, V. G. Zakrzewski, J. Gao, N. Rega, G. Zheng, W. Liang, M. Hada, M. Ehara, K. Toyota, R. Fukuda, J. Hasegawa, M. Ishida, T. Nakajima, Y. Honda, O. Kitao, H. Nakai, T. Vreven, K. Throssell, J. A. Montgomery, J. E. P. Jr., F. Ogliaro, M. Bearpark, J. J. Heyd, E. Brothers, K. N. Kudin, V. N. Staroverov, T. Keith, R. Kobayashi, J. Normand, K. Raghavachari, A. Rendell, J. C. Burant, S. S. Iyengar, J. Tomasi, M. Cossi, J. M. Millam, M. Klene, C. Adamo, R. Cammi, J. W. Ochterski, R. L. Martin, K. Morokuma, O. Farkas, J. B. Foresman and D. J. Fox, *https://gaussian.com/g09citation/*, 2009, preprint, https://gaussian.com/g09citation/:A.02.

14 Y. Zhao and D. G. Truhlar, *Theor Chem Acc*, 2008, **120**, 215–241.

15 D. E. Woon and T. H. Dunning, *J Chem Phys*, 1995, **103**, 4572–4585.

16 A. D. Becke, *J Chem Phys*, 1993, **98**, 5648–5652.

17 T. Le Bahers, C. Adamo and I. Ciofini, *J Chem Theory Comput*, 2011, **7**, 2498–2506.

18 E. Cancès, B. Mennucci and J. Tomasi, *J Chem Phys*, 1997, **107**, 3032–3041.

19 J. Tomasi, B. Mennucci and E. Cancès, *Journal of Molecular Structure: THEOCHEM*, 1999, **464**, 211–226.

20 T. Baldacchini, C. N. LaFratta, R. A. Farrer, M. C. Teich, B. E. A. Saleh, M. J. Naughton and J. T. Fourkas, *J Appl Phys*, 2004, **95**, 6072–6076.